Journal of Scientific Research & Reports

Volume 29, Issue 1, Page 14-25, 2023; Article no.JSRR.96124
ISSN: 2320-0227

Heat Transfer Analysis of Silver-water Nanofluid Flow over Stretching Cylinder Subjected to Multiple Convective Conditions over Stretching Sheet and Stretching Cylinder

Pardeep Kumar [a], Hemant Poonia [a] and Pavitra Kumari [a*]

[a] *Department of Mathematics and Statistics, Chaudhary Charan Singh Haryana Agricultural University, Hisar, 125004, Haryana, India.*

Authors' contributions

This work was carried out in collaboration among all authors. All authors read and approved the final manuscript.

Article Information

DOI: 10.9734/JSRR/2023/v29i11722

Open Peer Review History:
This journal follows the Advanced Open Peer Review policy. Identity of the Reviewers, Editor(s) and additional Reviewers, peer review comments, different versions of the manuscript, comments of the editors, etc are available here: https://www.sdiarticle5.com/review-history/96124

Original Research Article

Received: 24/11/2022
Accepted: 31/01/2023
Published: 04/02/2023

ABSTRACT

Tiny particles are essential in electronics, heat exchangers, nanotechnology, and materials science because of their exceptional thermal conductivity and unique properties. The study investigate the MHD flow over a stretching cylinder containing silver-water nanofluid in the presence of a magnetic field under multiple convective boundary conditions over stretching sheet and stretching cylinder. A system of PDEs is reduced to a solvable system of ODEs by applying a suitable similarity transformation. We employ the Runga Kutta method along with shooting procedure to solve the flow, heat, and mass transfer equations along with boundary conditions.

**Corresponding author: E-mail: yadavbunty67@gmail.com;*

The results obtained from MATLAB codes are compared with previously published results of the same nature in limiting case. In this model, we made a comparison between the stretching cylinder and a flat sheet and those are represented via graphically. Numerical results of skin-friction coefficient and local Nusselt are systematized in the form of tables for sheet and stretching cylinder. The plots illustrate the effect of different dimensionless parameters on velocity, temperature, and concentration profiles. Significant role of Biot number on temperature and concentration profile was observed. Nusselt number increases with Bi and Pr but decreases with M. The skin friction is enhanced with M but decrease with λ.

Keywords: MHD; mixed convection; nanofluid; numerical analysis.

2010 MSC: 00-01, 99-00.

1 INTRODUCTION

The addition of nanoparticles to a base fluid, the elasticity of surfaces, the application of a magnetic flux, the addition of artificial surface roughness, the attachment of fins, and the insertion of barriers are mechanisms for enhancing passive heat transfer. Over the past few decades, scientists have worked very hard to create novel nanofluids that perform better. A hybrid nanofluid is a nanofluid that contains two or more nanoparticles. Numerous studies have demonstrated that hybrid nanofluids are superior to single nanofluids. Compared to hybrid nanoparticles, single nanoparticles had a less impact on temperature dispersion. Choi and Eastman [1] first identified the unique heat transmission and cooling properties of nanofluid. They found that the physical and chemical characteristics of the standard fluid and nanofluid are different, and proposed nanofluid as a suspension of nanoparticles (1-100 nm in size) in the base fluid. Bagh et al. [2] investigated the 3D convective heat transfer features of a magneto hydrodynamic nanofluid flow that comprised oxytactic motile microorganisms and nanoparticles and flowed through a rotating cone. The impact of thermal energy, velocity profiles, and concentration slip on an MHD flow of a nanofluid constrained by Sohaib et al. [3] over the stretching surface. Williamson nanofluid flow with the effects of thermal radiation and thermo-diffusion through a porous stretching/shri-nking sheet was examined by Bhatti and Rashidi [4]. Alilat et al.[5] explain the Inertial and Porosity Effects on Dupuit-Darcy Natural Convection of Cu-Water Nanofluid Saturated High Thermal Conductive Porous Many researchers have been concentrating on the creation and utilisation of nanofluids in various areas, especially in the case of stretching sheets [6, 7, 8, 9] and cylinders [10, 11, 12]. Inertial effects on the hydromagnetic natural convection of SWCNT-water nanofluid-saturated inclined rectangular porous medium studed by Alilat et al. [5]. Ibrahim et al. [13] examined the MHD Williamson liquid over a stretching cylinder with the importance of activation energy. Gouran et al. [14] examined the effects of thermal radiation on nanofluid flow between two circular cylinders under the influence of a magnetic field. In contrast to the conventional Fourier's equation of heat conduction, Dogonchi and Ganji [15] investigated an unstable squeezing MHD nanofluid flow and heat transfer between two parallel plates in the presence of thermal radiation impact. Theoretical analysis was done by Abdelhafez et al. [16] on the Magnetohydrodynamic (MHD) flow over a nanofluid through a porous medium induced by a solar energy stretching sheet. Arifin et al.[17] examined the magnetohydrodynamic, suctional, and Joule heating effects on the horizontally stretched/shrinking layer as well as the dynamics flow and thermal expansion of the hybrid Cu Al2O3/water nanofluid. The flow of third-grade nanofluid through a stretched cylinder was discussed by Shafiq et al. [18]. Maxwell Nanofluids FEM Simulation of the Effects of Suction/Injection on the Dynamics of Rotatory Fluid Subjected to Bioconvection, Lorentz, and Coriolis Forces [19]. The bioconvection analysis for nanofluid flow in a square cavity was carried out by Mansour et al. [20]. In a porous channel with such a mass flow characteristic, Sharmaet al. [21] investigated the effects of buoyancy and flow rate over Sisko nanoparticles across a vertical stretched surface. The optimization of heat transfer in thermally convective micropolar-based nanofluid flow by the influence of nanoparticle's diameter and nanolayer via stretching sheet: sensitivity analysis approach is describe by Ali et al. [22].Heat and mass transfer using magneto-micropolar electrically conducting nanofluid flow over a linearly stretching sheet with convective boundary conditions is studied by Bilal [23]. He includes joule heating effects and non-linear thermal radiation in the energy equation. Thermal radiation and electrical magnetohydrodynamics phenomena have also been

studied in an infinitely spinning disk's convective boundary layer flow of a nanofluid [24]. Yahya Ali Rothan [25] examines the use of nanotechnology and the impact of FHD on the flow of fluid inside a container. Iron oxide and water make up the carrier fluid, and a homogeneous model was used to infer the features. Tiny particles are essential in electronics, heat exchangers, nanotechnology, and materials science because of their exceptional thermal conductivity and unique properties [26, 27]. The magnetohydrodynamic Ag/water nanofluid is examined in a two-dimensional continuous flow over a stretching cylinder or flat sheet. The set of higher-order partial equations was transmuted to lower-order differential equations and numerically solved under physically realistic boundary conditions. This flow regime can be found in technological mechanisms for mechanical means such as shrink packing, shrinking film, shrinkage wrapping, and thermal procedure. The fluctuating trends of physical outcomes are particularly noticeable for velocity, temperature functions, and the results are graphed with other physical factors such as stratification, concentration, and buoyancy factors. In this scenario, the current description goes ahead in pursuit of the responses to the following quarries.

2 PHYSICAL PATTERN AND INTERPRETATION

The magneto hydrodynamic Ag/water nanofluid is examined in a two-dimensional continuous flow over a stretching cylinder or flat sheet sketched in Fig.1. This section shows a mathematical model for analyzing heat and mass transfer in a two-dimensional nanofluid flow towards a cylinder with radius R with free stream velocity U_∞ has been consider. The impacts of convective boundary conditions are included in this paper to broaden the scope of the research. Let free stream velocity $u_w = \frac{ax}{l}$ flow over the cylinder, where a is a positive constant. The coordination system takes into consideration the x-axis along the cylinder's surface and the r along the axial direction. The surface temperature is the result of convective heating from a hot fluid, expressed with T and h_f is the thermal efficiency. The thermo-physical properties of nanoparticles are shown in Table 1. The Tiwari and Das model have been taken into consideration. The governing equations are given in light of the above assumptions [28, 29, 30].

$$\frac{\partial(ru)}{\partial x} + \frac{\partial(rv)}{\partial r} = 0 \tag{1}$$

$$u\frac{\partial u}{\partial x} + v\frac{\partial u}{\partial r} = \frac{\mu_{nf}}{\rho_{nf}}\left(\frac{\partial^2 u}{\partial r^2} + \frac{1}{r}\frac{\partial u}{\partial r}\right) - \frac{\sigma_{nf}B_0^2}{\rho_{nf}}u + \left[\frac{(\rho\beta)}{\rho_{nf}}g(T - T_\infty)\right] \tag{2}$$

$$(\rho C_p)_{nf}\left(u\frac{\partial T}{\partial x} + v\frac{\partial T}{\partial r}\right) = \kappa_{nf}\left(\frac{\partial^2 T}{\partial r^2} + \frac{1}{r}\frac{\partial T}{\partial r}\right) \tag{3}$$

$$u\frac{\partial C}{\partial x} + v\frac{\partial C}{\partial r} = D_m\left(\frac{\partial^2 C}{\partial r^2} + \frac{1}{r}\frac{\partial C}{\partial r}\right) + \frac{D_m k_t}{T_m}\left(\frac{\partial^2 T}{\partial r^2} + \frac{1}{r}\frac{\partial T}{\partial r}\right) \tag{4}$$

According to the problem's geometry, the boundary conditions can be divided into the preceeding classes:

$$\left.\begin{array}{ll} (a) & u = U_w = 0, \quad v = 0, \quad \kappa_{nf}\dfrac{\partial T}{\partial r} = -h_{nf}\{T_w - T\}, \quad D_n\dfrac{\partial C}{\partial r} = -h_f\{C_w - C\} at \quad r = R \\ (b) & u \to u_w = \dfrac{ax}{l}, \quad T \to T_\infty, \quad C \to C_\infty, \quad at \quad r \to \infty \end{array}\right\} \tag{5}$$

Where u and v are the velocity components along x and r directions. And $\{\kappa/(\rho C_p)_f\}$, the thermal conductivity of fluid is κ and specific heat is C_p. The fluid temperature is (T), and (B_0) is the magnetic field parameter, dynamic viscosity (μ) and the density of the based fluid is (ρ). With the exception of density changes that create a thermal buoyancy force retains consistent characteristics.

Table 2 shows that the subscripts f_s and n_f stand for fluid, solid nanoparticles of Ag, and nanofluid, respectively. By introducing the non-dimensional variables below, the elaborated problem's complexity is simplified.:

$$\left.\begin{array}{r} \Phi(x,r) = R\sqrt{u_w\nu_f x}F(\xi),\ \xi = \dfrac{r^2 - R^2}{2R}\left(\dfrac{u_w}{\nu_f x}\right)^{\frac{1}{2}},\ u_w = \dfrac{ax}{l}\ \theta(\xi) = \dfrac{T - T_\infty}{T_w - T_\infty}, \\ ru = \dfrac{\partial\Phi}{\partial r}, \psi(\xi) = \dfrac{C - C_\infty}{C_w - C_\infty},\ rv = -\dfrac{\partial\Phi}{\partial x}, \end{array}\right\} \tag{6}$$

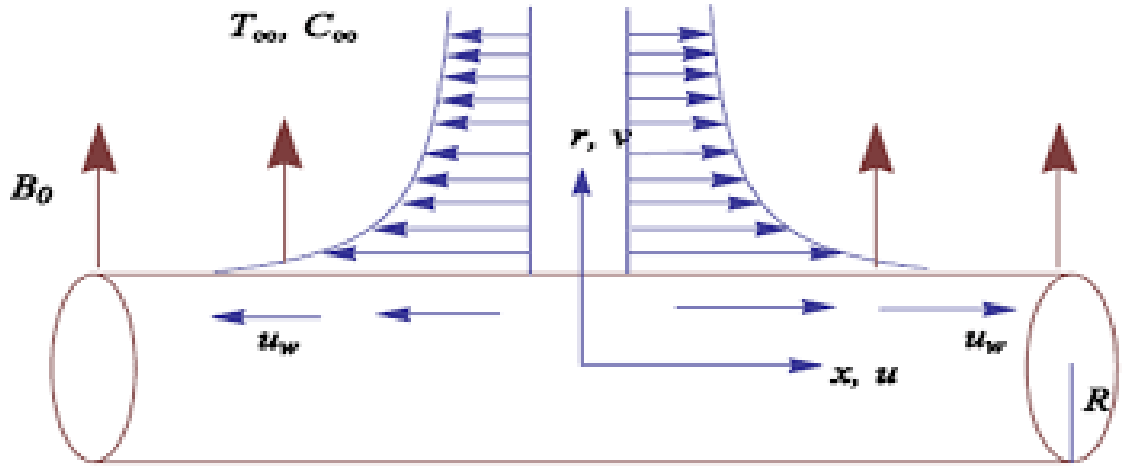

Fig. 1. Physical flow diagram

Table 1. The physical Properties [31, 32].

Physical properties	$\rho(kg.m^{-3})$	$C_p(J/kg \cdot K)$	$\kappa(W/m \cdot K)$	$\sigma \times 10^5\ k^{-1}$
H_2O	0997.1	4179.0	00.613	2.1 $\times 10^{-4}$
Ag	10500	235.00	429.00	1.89 $\times 10^{-5}$

Table 2. Thermophysical properties of water and nanofluid [33, 34]

Properties	Nanofluid
Density (ρ)	$\frac{\rho_{nf}}{\rho_f} = (1-\phi) + \frac{\rho_s}{\rho_f}\phi$
Viscosity (μ)	$\mu_{n_f} = \frac{\mu_f}{(1-\phi)^{2.5}}$
Heat capacity (ρC_p)	$\frac{(\rho C_p)_{nf}}{(\rho C_p)_f} = (1-\phi) + \frac{(\rho C_p)_s}{(\rho C_p)_f}\phi$
Electrical conductivity (σ)	$\frac{\sigma_{nf}}{\sigma_f} = 1 + \frac{3(\sigma-1)\phi}{(\sigma+2)-(\sigma-1)\phi}$

Here the stream functions Φ and ξ are dimensionless. In order to satisfy equation 1, the Φ stream function is typically defined. Then, using the similarity vectors (6) mentioned above, the non linear partial differential equations (2-4) are transformed as follows:

$$(2\xi\Gamma + 1)F''' + 2\Gamma F'' + \frac{1}{B_1}\lambda\theta + \frac{B_2}{B_1}\left[1 + FF'' - \left(F'\right)^2\right] - \frac{MB_3}{B_1}F' = 0 \tag{7}$$

$$\left[(2\xi\Gamma + 1)\theta'' + 2\Gamma\theta'\right] + \frac{B_5}{B_4}P_r\left[F\theta'\right] = 0 \tag{8}$$

$$(1 + 2\xi\Gamma)\psi'' + (LeF + 2\Gamma)\psi' + Sr\left[(1 + 2\xi\Gamma)\theta'' + 2\Gamma\theta'\right] = 0 \tag{9}$$

$$\tag{10}$$

Moreover, the modified boundary conditions are as follows;

$$\left.\begin{array}{l} F(\xi) = 0,\ F'(\xi) = 0,\ \theta'(\xi) = -Bi\{1 - \theta(0)\},\ \psi'(\xi) = -Bi_2\{1 - \psi(0)\},\ at\ \xi = 0 \\ F'(\xi) \to 1,\ \theta(\xi) \to 0,\ \psi(\xi) \to 0, at\ \xi \to \infty \end{array}\right\} \tag{11}$$

and the transformed boundary conditions are described as; The thermos-physical factors are explained such as; [35]

$$B_1 = (1-\phi)^{2.5}, \quad B_2 = \{(1-\phi) + \frac{\rho_s}{\rho_f}\phi\} \qquad B_3 = \frac{\sigma_{nf}}{\sigma_f} = 1 + \frac{3(\sigma-1)\phi}{(\sigma+2)-(\sigma-1)\phi}$$

$$B_5 = \frac{k_s + (s_f-1)k_{bf} - (s_f-1)(k_f-k_s)\phi}{k_s + (s_f-1)k_{bf} + (k_f-k_s)\phi}$$

$$B_4 = \frac{(\rho C_p)_{nf}}{(\rho C_p)_f} = (1-\phi) + \frac{(\rho C_p)_s}{(\rho C_p)_f}\phi$$

3 PHYSICAL QUANTITIES

The various involving parameters in equations (08) to (13) are also described, as are the numerous participating parameters are Prandtl number (P_r), Magnetic parameter (M), traditional Lewis number (L_e), Biot number (B_i), Lewis number (L_b), mixed convection parameter (λ), Grashof number (G_r), Reynolds number, (S_r) Soret number, thermally stratified variable (θ_t) and the curvature parameter (Γ).

$$\left.\begin{aligned} M = \frac{\sigma_f B^2{}_0 l}{\rho_f a},\ Sr = \frac{k_t(T_w - T_\infty)}{T_m(C_w - C_\infty)}, \\ Le = \frac{\mu_f}{\rho_f D_m}, \lambda = \frac{G_r}{R_E},\ G_r = \frac{\beta_f g(T_w - T_\infty l^3)}{\nu_f^2},\ R_e = \frac{U - wl}{\nu_f},\ Pr = \frac{\mu_f}{\rho_f \alpha_f} \\ \Gamma = \frac{1}{R}\sqrt{\frac{\mu_f l}{\rho_f a}},\ Bi = \frac{Rh_{nf}}{(\kappa_{nf})r}\sqrt{\frac{l\nu_f}{a}},\ \alpha_f = \frac{\kappa_f}{(\rho c)_f} \end{aligned}\right\}$$

4 ENGINEERING QUANTITIES

The requisite aspects of engineering interest skin friction coefficient C_{fx}, local Nusselt number Nu_x, local Sherwood number Sh_x, and the bioconvective number B_1 are the practical interest quantities as follows:

$$C_{fx} = \frac{2\mu_{nf}}{\rho U_\infty^2}\left(\frac{\partial u}{\partial r}\right)_{r=R}, \quad Nu_x = \frac{x\kappa_{nf}}{\kappa(T_w - T_\infty)}\left(\frac{\partial T}{\partial r}\right)_{r=R} \tag{12}$$

In view of the above similarity transformation functions (8), can be calculated as:

$$C_{fx} = \sqrt{Re_x}C_f = 2B_1\frac{d^2F(0)}{d\zeta^2}, \quad \frac{Nu_x}{\sqrt{Re_x}} = -1B_5\{\theta'(0)\}, \quad \frac{Sh_x}{\sqrt{Re_x}} = -\phi'(0),$$

where $Re_x = xu_w/\nu_f$ is the local Reynold's number.

5 EXECUTION OF METHODOLOGY

The system of ODE's is numerically solved by the RK technique. In which estimates the mathematical solutions numerically using an adaptive Runge-Kutta method (for solutions) in Matlab and for shooting we implemented the Newton-Raphson method [36]. We do this by first assuming:

$f_1 = \Pi_1,\ \ f_1' = \Pi_2,\ \ f_1'' = \Pi_3$
$\theta = \Pi_4,\ \ \theta' = \Pi_5, \Phi = \Pi_6,\ \ \Phi' = \Pi_7,$
$\zeta = \Pi_8,\ \ \zeta' = \Pi_9$

$\Pi_1' = \Pi_2$
$\Pi_2' = \Pi_3$
$\Pi_3' = \frac{-1}{(1+2\Gamma\xi)}[2\Gamma\Pi_3 + \frac{B2}{B1}(1 + \Pi_1\Pi_3 - \Pi_2^2) + \frac{B3}{B1}\lambda\Pi_4 - \frac{MB_3}{B1}\Pi_2]$
$\Pi_4' = \Pi_5$
$\Pi_5' = \frac{1}{(B_4(1+2\Gamma\xi))}[2B_4\Gamma\Pi_5 + B_5(P_r)(\Pi_1\Pi_5)]$
$\Pi_6' = \Pi_7$
$\Pi_7' = \frac{-1}{(1+2\Gamma\xi)}[(2\Gamma + L_e\Pi_1)\Pi_7 + S_r(1 + 2\Gamma\xi)(\Pi_5') + 2\Gamma\Pi_5)]$

with

$\Pi_1(0) = 0,\ \Pi2(0) = 1,\ \Pi_3(0) = \Delta_1,\ \Pi_4(0) = \Delta_2,\ \Pi_5(0) = Bi(1 + \Pi_4(0)),\ \Pi_7(0) = Bi_2(1 + \Pi_6(0))$
$\Pi_7(0) = \Delta_3,\ \Pi_8(0) = 1,$

where $\Delta_1,\ \Delta_2,\ \Delta_3,$ are calculated with an appropriate initial guess using the Newton Raphson technique. The numerical technique (Runge Kutta) was validated, and it was found to have an excellent agreement in Table3.

Table 3. Comparison of $-\theta'(0)$ for different values of P_r and other parameters are constant

P_r	Gorla and Sidawi [37]	Khan and pop [38]	Hamad [39]	Present result
00.02	00.1691	00.1691	0.16908	0.169087
00.70	00.5349	00.4539	0.45395	0.453912
02.08	00.9114	00.9113	0.91134	0.911357
07.00	01.8905	01.8954	1.89545	1.895405
20.00	03.3539	03.3539	3.35392	3.353929
70.00	06.4622	06.4622	6.46220	6.462364

6 RESULTS AND DISCUSSION

Table 4 shows the numerical validation and the comparison of the present study with previous results. The stimulus of various parameters has an impact on momentum profile $F(\xi)$, thermal distribution $\theta(\xi)$, nanoparticle concentration profile $\psi(\xi)$ is investigated for both stretching cylinder and a flat sheet scenario, which is revealed in Figs. (2(a-b)-6(a-b)) It is remarked that all graphical analysis is performed for flow confined by stretched cylinder $(\Gamma = 0.5)$ and flow due to flat plate $(\Gamma = 0.0)$. To accomplish this purpose, figures and tables are presented. Fig. (2a) revealed magnetic field qualities on the velocity profile. we can see from this diagram that the dimensionless velocity falls as the magnetic parameter increases for both surfaces. The increasing change in F' is comparatively more progressive for flat plate configuration. It is due to impact of curvature parameter on the velocity profile. In fact for higher values of curvature parameter, the radius of cylinder increases which enhances fluid flow. Physical resion for magnetic parameter describe as the Lorentz force is induced by the presence of a transverse magnetic field in an electrically conducting liquid, which slows the fluid' s flow within the boundary layer area. The impact of the mixed convection parameter λ on the velocity profile is shown in Fig. (2b). The velocity profile enhanced with λ whereas thermal layer decreases for both sheet and cylinder surfaces. The increasing change in F' is comparatively more progressive for flat plate configuration. Physically the ratio of inertial to buoyant forces is the mixed convection parameter, an increase in λcorrelates to increased thermal buoyancy forces, which improves velocity profiles. Figs. (3a-3b) depicts the relationship between the magnetic parameter with the concentration and temperature distributions for both stretchable cylinder and sheet cases. As the magnetic parameter' s values rise, the thermal boundary layer and concentration layer become thicker. The Lorentz drag, which acts as an opposing force, helps to increase the frictional heating between the fluid layers, which results in the release of energy in the form of heat. As a result, the thermal boundary layer thickens. The Fig. (4a) depict the dropping impact of the velocity profile with Prandtl number Pr for both stretching cylinder and a flat sheet scenario. The higher the Pr, the more viscous the fluid, causing the boundary layer to thicken, reducing shear stress

Table 4. The Comparison of Nusselt number (Nu_x) and skin friction coefficient (Cf_x) for Stretching Sheet and Stretching cylinder with different values of M, λ, Pr, Bi while other parameters remain fixed

2*M	2*λ	2*Pr	2*Bi	Stretching Sheet $Nu_x Re_x^{-1/2}$	Stretching Sheet $\frac{1}{2}C_f x_x^{-1/2}$	Stretching Cylinder $Nu_x Re_x^{-1/2}$	Stretching Cylinder $\frac{1}{2}C_f x_x^{-1/2}$
0.1	0.1	0.5	0.1	0.209526	0.656857	0.204496	0.822342
0.3	-	-	-	0.206775	0.748592	0.203875	0.885590
0.5	-	-	-	0.203778	0.862956	0.201078	0.993657
0.3	0.2	0.5	0.1	0.205185	0.773839	0.202783	0.908940
-	0.4	-	-	0.205556	0.761340	0.203059	0.896035
-	0.6	-	-	0.206154	0.750920	0.203754	0.885141
0.3	0.2	0.1	0.1	0.302991	-1.057740	0.252993	0.787404
-	-	0.3	-	0.377056	0.877402	0.287054	0.787404
-	-	0.5	-	0.390285	0.877403	0.310283	0.784041
-	-	-	0.1	0.237241	0.877403	0.207278	0.677395
-	-	-	0.2	0.373043	0.577409	0.273065	0.677409
-	-	-	0.5	0.572047	0.577402	0.044202	0.677410

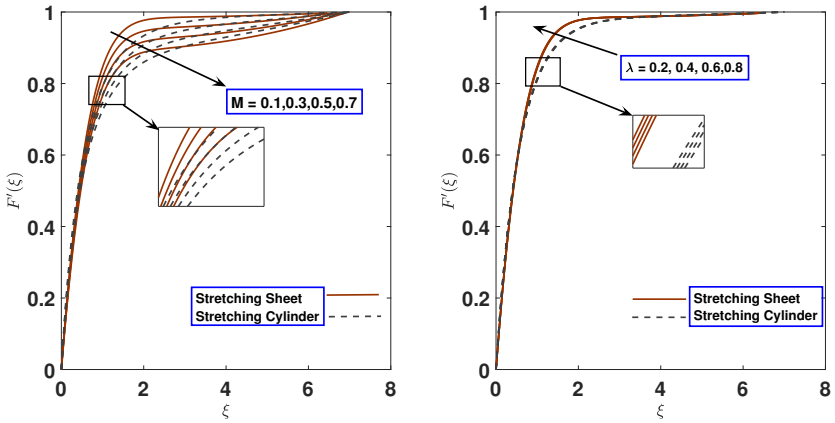

Fig. 2. (a-b) Fluctuation of Velocity profile along with variation of M and λ

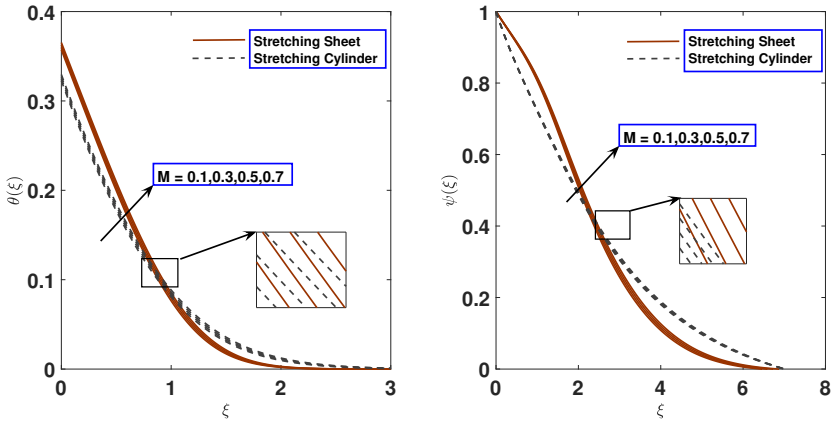

Fig. 3. (a-b) Fluctuation of Temperature profiles and concentration profile along with M

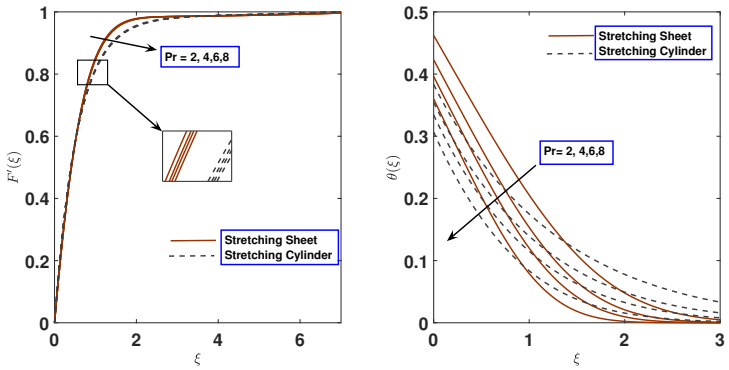

Fig. 4. (a-b) Variation in velocity and temperature profile against η for different values of Pr

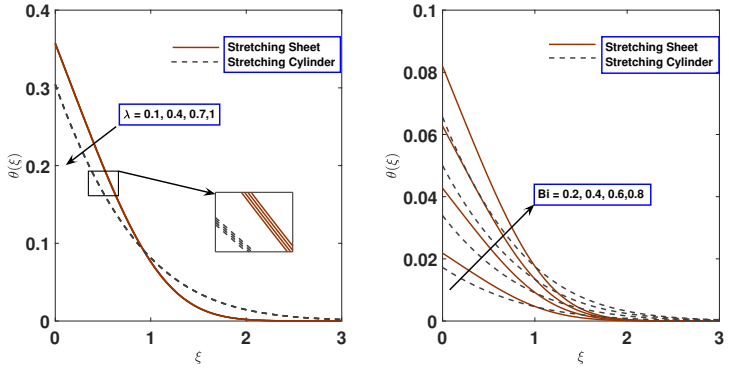

Fig. 5. (a-b) Variation in velocity profile against η for different values of R_d and λ_θ

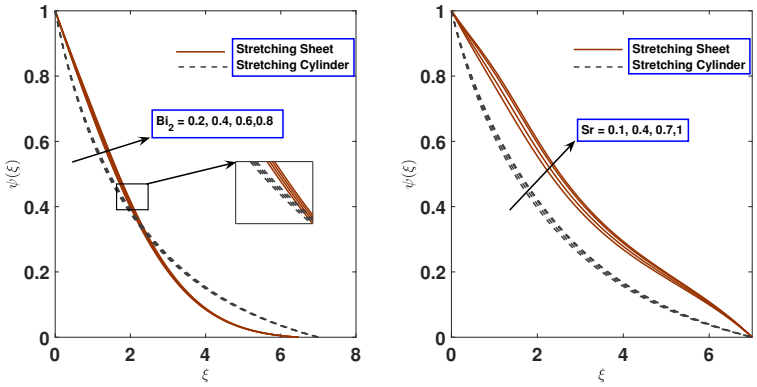

Fig. 6. (a-b) Fluctuation of concentration profiles along with different values of Bi_2 and Sr

and therefore retarding the nano fluid' s flow. Fig. (4b), describe the influence of Prandtl number Pr on nanoparticle temperature. Again, results are prepared by stretched cylinder $\Gamma = 0.5$ and flow due to flat plate $\Gamma = 0.0$. The profile decreases with Pr. Physically the Prandtl number is a non-dimension quantity, defined as the ratio of two quantities momentum and thermal diffusivity. Thermal diffusivity diminishes when Pr rises which further gives a drop-in boundary layer thickness and temperature. The impact of the mixed convection parameter λ on the temperature profile is shown in Fig. (5a). The thermal layer decreases

for both sheet and cylinder surfaces. Fig. (5b) illustrates the observation that the thermal layer and becomes a more noticeable characteristic of fluid layers with rising Biot number Bi both stretchable cylinder and sheet cases. Both profiles enhanced with Bi. Physically convective heating occurs at the sheet more frequently and intensifies as Bi increases, increasing the temperature. If the variation is greater, the thermal influence can reach the quiescent fluid. In addition, as the fluid temperature rises, the stretched sheet's right-hand side Biot number increases, decreasing its thermal resistance and increasing convectional heat transfer. Fig. (6a) illustrates the observation that the concentration profile becomes a more noticeable characteristic of fluid layers with rising concentration Biot number Bi_2 both stretchable cylinder and sheet cases. It can be noticed that the greater value of thermal Biot number Bi_2 improves the concentration field. In fact, concentration Biot number is physically related to the coefficient of mass transfer which is responsible to improve the concentration profile. The profiles enhanced with Bi_2. A decrease in concentration profile can be observed with increased Sr parameter values both stretchable cylinder and sheet cases is shown in Fig. (6b). Physically ratio of viscosity to mass diffusivity is known as Schmidt number. When Schmidt number increases then mass diffusivity decreases. Ultimate there is reduction in fluid concentration. Table (4) elucidate the variation of pertinent parameters on heat transfer and drag coefficient. Further a decreasing effects on the skin coefficient with increasing in magnetic field M and λ but remains constant with $P_r, and B_i$. While nusselt number reinforce with increasing in parameters P_r, Biot number B_i and λ where as decreasing function of magnetic field M. Also we compare the stretching sheet with that of the stretching cylinder.

7 CONCLUDING REMARKS

In this paper, presents the stretching cylinder and flat sheet along with the multiple convective boundaries condition have been analyzed. Furthermore, the Prandtl number, velocity, and temperature for both stretching cylinder and flate sheet based Ag/water nanofluids are provided and compared in this work. Nonlinear ordinary differential equations are attained by proposing relevant similarity transformations on partial differential equations. These non-dimensional ordinary differential equations are then converted to the system of first order ODEs and solved numerically Rk method along wuth shooting method. Graphical results are compared and displayed for both the stretching cylinder and stretching sheet. The impact of the influential parameters on velocities, skin friction, temperature, Nusselt number, and concentration has been conceived. The following section summarizes the significant results relating to the variable nature of physical quantities as influenced by the governing parameters.

- Thinning of concentration field relates to increasing values of thermal stratification parameter S_r and with the inclination of values the heat transfer rate accelerates.
- When a stretching cylinder is compared to a flat sheet, the velocity is noticeably greater.
- The nanofluid velocity improved with velocity ratio parameter while magnetic constant reduce the velocity.
- Wall shear stress increases and rate of heat transfer decreases on the surface for the increasing value of curvature parameter.
- The thickness of thermal boundary layers and heat transfer rates increased due to increase in magnetic field parameters and Biot number.
- Nusselt number reinforce with increasing in parameters P_r, Biot number B_i and λ where as decreasing function of magnetic field M.
- Enhancement of velocity, temperature and concentration profile for the stretching cylinder is much greater than stretching sheet.
- it is observed that skin friction has greater value in case of stretching cylinder that stretching sheet whereas opposite behaviour of Nusselt number.

COMPETING INTERESTS

Authors have declared that no competing interests exist.

REFERENCES

[1] Choi SUS, Eastman JA. Enhancing Thermal Conductivity of Fluids with Nanoparticles. Argonne National Lab.(ANL), Argonne, IL (United States); 1995.

[2] Ali L, Liu X, Ali B, Mujeed S, Abdal S. Finite element simulation of multi-slip effects on unsteady MHD bioconvective micropolar nanofluid

flow over a sheet with solutal and thermal convective boundary conditions. Coatings. 2019;9(12):842.

[3] Abdal S, Ali B, Younas S, Ali L, Mariam A. Thermo-diffusion and multislip effects on MHD mixed convection unsteady flow of micropolar nanofluid over a shrinking/stretching sheet with radiation in the presence of heat source. Symmetry. 2019;12(1):49.

[4] Bhatti MM, Rashidi MM. Effects of thermo-diffusion and thermal radiation on Williamson nanofluid over a porous shrinking/stretching sheet. Journal of Molecular Liquids. 2016;221:567-573.

[5] Alilat, D and Alliche, M, Rebhi, Redha and Chamkha, Ali J. Inertial effects on the hydromagnetic natural convection of SWCNT-water nanofluid-saturated inclined rectangular porous medium. International Journal of Fluid Mechanics Research. 2020;47(5). Begel House Inc.

[6] Bilal M, Sagheer M, Hussain S. Three dimensional MHD upper-convected Maxwell nanofluid flow with nonlinear radiative heat flux. Alexandria engineering journal. 2018;57(3):1917-1925.

[7] Lozano-Steinmetz F, Martínez VA, Vasco DA, Sepúlveda-Mualin A, Singh DP. The Effect of Ag-Decoration on rGO/Water Nanofluid Thermal Conductivity and Viscosity. Nanomaterials. 2022;12(7):1095.

[8] Mir S, Abed AM, Akbari OA, et al. Effects of curvature existence, adding of nanoparticles and changing the circular minichannel shape on behavior of two-phase laminar mixed convection of Ag/water nanofluid. Alexandria Engineering Journal. 2023;66:707-730.

[9] Verma L, Meher R. Effect of heat transfer on Jeffery–Hamel Cu/Ag–water nanofluid flow with uncertain volume fraction using the double parametric fuzzy homotopy analysis method. The European Physical Journal Plus. 2022;137(3): 372.

[10] Adnan, Abbas W, Z. Bani-Fwaz M, Kenneth Asogwa K. Thermal efficiency of radiated tetra-hybrid nanofluid [(Al2O3-CuO-TiO2-Ag)/water] tetra under permeability effects over vertically aligned cylinder subject to magnetic field and combined convection. Science Progress. 2023;106(1):00368504221149797.

[11] Reddy NK, Swamy HAK, Sankar M, Jang B. MHD convective flow of Ag-TiO2 hybrid nanofluid in an inclined porous annulus with internal heat generation. Case Studies in Thermal Engineering. Published online 2023:102719.

[12] Ashraf MB, Tanveer A, Ulhaq S, Others. Effects of Cattaneo-Christov heat flux on MHD Jeffery nano fluid flow past a stretching cylinder. Journal of Magnetism and Magnetic Materials. 2023;565:170154.

[13] Ibrahim W, Negera M. The investigation of MHD Williamson nanofluid over stretching cylinder with the effect of activation energy. Advances in Mathematical Physics. 2020;2020.

[14] Gouran S, Mohsenian S, Ghasemi SE. Theoretical analysis on MHD nanofluid flow between two concentric cylinders using efficient computational techniques. Alexandria Engineering Journal. 2022;61(4):3237-3248.

[15] Dogonchi AS, Ganji DD. Impact of Cattaneo–Christov heat flux on MHD nanofluid flow and heat transfer between parallel plates considering thermal radiation effect. Journal of the Taiwan Institute of Chemical Engineers. 2017;80:52-63.

[16] Abdelhafez MA, Abd-Alla AM, Abo-Dahab SM. MHD convective non-Darcy flow of a nanofluid through a porous stretching sheet with thermal buoyancy and chemical reaction. Waves in Random and Complex Media. Published online 2022:1-18.

[17] Khashi'ie NS, Arifin NM, Nazar R, Hafidzuddin EH, Wahi N, Pop I. Magnetohydrodynamics (MHD) axisymmetric flow and heat transfer of a hybrid nanofluid past a radially permeable stretching/shrinking sheet with Joule heating. Chinese Journal of Physics. 2020;64:251-263.

[18] Shafiq A, Khan I, Rasool G, Seikh AH, Sherif ESM. Significance of double stratification in stagnation point flow of third-grade fluid towards a radiative stretching cylinder. Mathematics. 2019;7(11):1103.

[19] Ali L, Manan A, Ali B. Maxwell Nanofluids: FEM Simulation of the Effects of Suction/Injection on the Dynamics of Rotatory Fluid Subjected to Bioconvection, Lorentz, and Coriolis Forces. Nanomaterials. 2022;12(19):3453.

[20] Mansour MA, Rashad AM, Mallikarjuna B, Hussein AK, Aichouni M, Kolsi L. MHD mixed bioconvection in a square porous cavity filled by gyrotactic microorganisms. Int J Heat Technol. 2019;37(2):433-445.

[21] Sharma RK, Bisht A, Others. Effect of buoyancy and suction on Sisko nanofluid over a vertical stretching sheet in a porous medium with mass flux condition. Indian Journal of Pure & Applied Physics (IJPAP). 2020;58(3):178-188.

[22] Ali L, Kumar P, Iqbal Z, et al. Journal of Non-Equilibrium Thermodynamics. Published online 2023.
DOI:10.1515/jnet-2022-0064

[23] Bilal M. Micropolar flow of EMHD nanofluid with nonlinear thermal radiation and slip effects. Alexandria Engineering Journal. 2020;59(2):965-976.

[24] Kumar R, Singh S. Computational Analysis of EMHD Flow of Nanofluid Over a Rotating Disk with Convective Boundary Conditions: Buongiorno's Model. In: Advances in Fluid and Thermal Engineering. Springer; 2021:231-247.

[25] Rothan YA. Influence of magnetic force on physical treatment of nanofluid laminar flow developing numerical approach. International Journal of Modern Physics B. Published online 2022:2350134.

[26] Hashim, Hafeez M, Chu YM. Numerical simulation for heat and mass transport analysis for magnetic-nanofluids flow through stretchable convergent/divergent channels. International Journal of Modern Physics B. 2021;35(19):2150198.

[27] Usman, Ijaz Khan M, Ullah Khan S, Ghaffari A, Chu YM, Farooq S. A higher order slip flow of generalized Micropolar nanofluid with applications of motile microorganisms, nonlinear thermal radiation and activation energy. International Journal of Modern Physics B. 2021;35(07):2150095.

[28] Song YQ, Waqas H, Al-Khaled K, et al. Bioconvection analysis for Sutterby nanofluid over an axially stretched cylinder with melting heat transfer and variable thermal features: A Marangoni and solutal model. Alexandria Engineering Journal. 2021;60(5):4663-4675.

[29] Bilal S, Sohail M, Naz R, Malik MY. Dynamical and optimal procedure to analyze the exhibition of physical attributes imparted by Sutterby magneto-nanofluid in Darcy medium yielded by axially stretched cylinder. Canadian Journal of Physics. 2020;98(1):1-10.

[30] Waqas H, Naqvi SMRS, Alqarni MS, Muhammad T. Thermal transport in magnetized flow of hybrid nanofluids over a vertical stretching cylinder. Case Studies in Thermal Engineering. 2021;27: 101219.

[31] Hayat T, Nadeem S. Heat transfer enhancement with Ag–CuO/water hybrid nanofluid. Results in physics. 2017;7:2317-2324.

[32] Esfe MH, Saedodin S, Biglari M, Rostamian H. An experimental study on thermophysical properties and heat transfer characteristics of low volume concentrations of Ag-water nanofluid. International Communications in Heat and Mass Transfer. 2016;74:91-97.

[33] Ghadikolaei SS, Yassari M, Sadeghi H, Hosseinzadeh K, Ganji DD. Investigation on thermophysical properties of Tio2–Cu/H2O hybrid nanofluid transport dependent on shape factor in MHD stagnation point flow. Powder technology. 2017;322:428-438.

[34] Ghadikolaei SS, Gholinia M, Hoseini ME, Ganji DD. Natural convection MHD flow due to MoS2–Ag nanoparticles suspended in C2H6O2H2O hybrid base fluid with thermal radiation. Journal of the Taiwan Institute of Chemical Engineers. 2019;97:12-23.

[35] Tiwari RK, Das MK. Heat transfer augmentation in a two-sided lid-driven differentially heated square cavity utilizing nanofluids. International Journal of heat and Mass transfer. 2007;50(9-10):2002-2018.

[36] Kiusalaas J. Numerical Methods in Engineering with MATLAB®. Cambridge university press; 2005.

[37] Reddy Gorla RS, Sidawi I. Free convection on a vertical stretching surface with suction and blowing. Applied Scientific Research. 1994;52(3):247-257.

[38] Khan WA, Pop I. Boundary-layer flow of a nanofluid past a stretching sheet. International journal of heat and mass transfer. 2010;53(11-12):2477-2483.

[39] Hamad MAA. Analytical solution of natural convection flow of a nanofluid over a linearly stretching sheet in the presence of magnetic field. International communications in heat and mass transfer. 2011;38 (4): 487-492.

Peer-review history:
The peer review history for this paper can be accessed here:
https://www.sdiarticle5.com/review-history/96124